Insights from Control Theory into Deep Brain Stimulation for Relief from Parkinson's Disease

Clare M. Davidson*, Annraoi M. de Paor*, and Madeleine M. Lowery*

*School of Electrical, Electronic and Communications Engineering, National University of Ireland, Dublin (UCD), Belfield, Dublin 4, Ireland, *e-mail*: annraoi.depaor@ucd.ie

***Abstract*—Using ideas from control theory. i.e., the root locus method, Lyapunov's theorem of the first approximation, the describing function, Nyquist stability theory and the concept of the equivalent nonlinearity associated with dither injection in a nonlinear feedback loop, the phenomenon of quenching of pathological neural oscillations by deep brain stimulation is explored. The model used contains a second order unstable, linear, dynamical system, in a negative feedback loop with a nonlinearity comprising a linear gain in parallel with a "signed square". This mimics, what is referred to by Alim Louis Benabid, the great pioneer of deep brain stimulation as "excitation of inhibitory pathways that lead to functional inhibition". Describing function analysis is used to give a very close estimate of the inherent, almost sinusoidal oscillation, which is quenched by deep brain stimulation. The relationship between the critical amplitude of deep brain stimulation (expressed either in volts or milliamps) and the fractional pulse width needed for quenching the oscillation is derived. This is fitted as closely as possible to experimental results by Benabid *et al*., by minimizing a sum of squared error index.**

***Index Terms*—Deep brain stimulation, Parkinson's disease, nonlinear control theory, oscillation quenching, neural mass model**

I. Introduction

Dopamine is a neurotransmitter that regulates the activity of the basal ganglia - a group of nuclei in the brain involved in controlling voluntary movement. Parkinson's disease, chronic, progressive and neurological, is characterized by a loss of dopamine, leading to symptoms such as bradykinesia, akinesia, rigidity and tremor. Current drug treatments focus on either replenishing the level of dopamine or mimicking its action. However as the disease progresses, the increased dosage needed to suppress the symptoms can cause a number of unwanted side effects, such that drug treatment becomes no longer a viable option.

Deep brain stimulation (DBS) is now well established as an effective method of treating the symptoms of medically refractive Parkinson's disease [1]. DBS applied to treat Parkinson's disease is typically a high frequency (¿100Hz) charge-balanced pulse train applied most often to the subthalamic nucleus (STN) via surgically implanted electrodes. The choice of stimulation amplitude and pulse duration is usually made on the basis of a qualitative assessment by the physician of an individual patient's symptoms. Amplitudes ranging from 1 to 5 V (or from 0.2 to 10 mA) and pulse durations from 60 to 450 μs are found to be clinically effective [2], [3], [4]

Pathological firing occurs in the neurons of the basal ganglia in both human and animal models of Parkinson's disease. An increase in spontaneous firing rate and periodic oscillatory activity is typically recorded [5], [6], [7], [8]. One prominent feedback loop in the basal ganglia is formed by the STN and the globus pallidus pars externa (GPe). It has been proposed as one (but not the only) source of these pathological oscillations. This proposal is supported by the study of an *in vitro* model by Plenz and Kital [9], which suggests that this loop can form a central basal ganglia pacemaker. Alternative possibilities are that the STN or GPe, or other centres can also generate oscillations due to internal interactions, or that cortical input to the STN drives the oscillations. DBS relieves many of the motor symptoms of Parkinson's disease [1]. One hypothesis is that it does this by quenching pathological neuronal oscillations that arise as a result of dopamine depletion. The exact mode of action of DBS, however, remains open to debate.

The injection of high frequency dither to modify the properties of a non-linear system is a well established engineering tool [10]. The resemblance of DBS quenching pathological oscillations in the STN-GPe or other relevant networks to the concept of 'high-frequency' dither injection being used to quench 'low-frequency' oscillations in nonlinear control feedback loops has previously been explored using a neural-mass type model of the basal ganglia [11]. The model initially developed in [11], which is of fourth order and contains two nonlinearities mirrored the idea that oscillation arises in the STN-GPe loop. It has been simplified since to a feedback loop containing a second order linear system and a single nonlinearity, which can represent a single group of neurons such as the STN [12]. This follows the demonstration by Rosenblum and Pikovsky[5] that the local field potential of a spontaneously oscillating family of interconnected neurons grows in accordance with second order dynamics.

Two complementary versions of the model have been developed in our studies, Model A and Model B, shown on Fig.1. Model A was presented and analyzed in [12], and Model B is discussed here. The duality of the models is noteworthy. In Model A the second order system in the neural mass model is asymptotically stable, and has a saturating type nonlinearity (an embodiment of the sigmoid found in many living control systems) in a positive feedback loop. The DBS signal reduces the effective gain of the sigmoid, thus giving what Benabid terms "jamming" of the loop. On the other hand, Model B contains an inherently unstable second order system with an unbounded nonlinearity (the signed square) in

978-1-4673-1179-3/12/$31.00 ©2012 IEEE

a negative feedback loop. In this case the effective gain of the nonlinearity is increased by DBS, in accord with what Benabid calls increased "excitation of inhibitory pathways" [13].

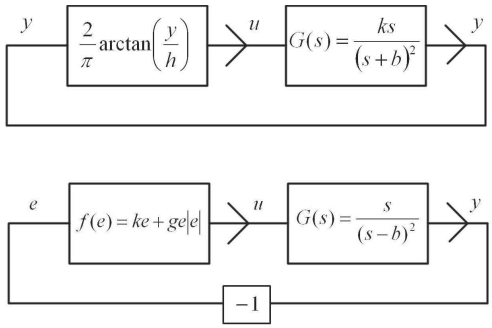

Fig. 1. The system considered. Two complementary models - Model A (upper diagram) and Model B.

The concordance of both models with experimental results by Benabid *et al.* [1] is close enough to encourage further exploration. This reinforces the value of "neural mass modeling"[14], in which the complexity of the system is reduced as much as possible, by concentrating on a signal associated with the action of neurons *en masse*, such as the Local Field Potential (LFP) measured, with respect to a distant reference, by an extracellular electrode located in the vicinity of the neurons of interest. Rosenblum and Pikovsky [5] have shown that in a group of 2000 neurons with complex firing patterns, the LFP evolves in accordance with second order dynamics. The expectation is that insight gained into the mode of action of DBS in these systems of minimum complexity will be valuable in a clinical setting, leading, for example, to synthesis of stimulating waveforms which reduce as much as possible (subject to clinical constraints) the power consumption of the chest-implanted stimulator, thus lengthening battery life, leading to longer intervals between operations needed to replace spent stimulators.

II. Application of Techniques from Control Theory

We shall now apply some ideas from the theory of automatic control to model B. Specifically we shall use:

1) The root locus method
2) Lyapunov's theorem of the first approximation
3) The describing function
4) Nyquist stability theory
5) The concept of the equivalent nonlinearity associated with dither injection in a nonlinear feedback loop.

The system to be considered is shown in Fig. 1.

We may, for small signal analysis, represent the nonlinear loop by an associated linear system, with the nonlinearity replaced by its slope at the origin:

$$\left.\frac{df}{de}\right|_{e=0} = k \tag{1}$$

The characteristic polynomial of the associated linear system is

$$P(s) = (s-b)^2 + ks \tag{2}$$

The root locus of $P(s)$, plotted for $0 \leqslant k < \infty$ comprises a circle of radius b centered at the origin on the $s = (\sigma, \omega)$ [15] plane as shown in Fig. 2, and portion of the real axis.

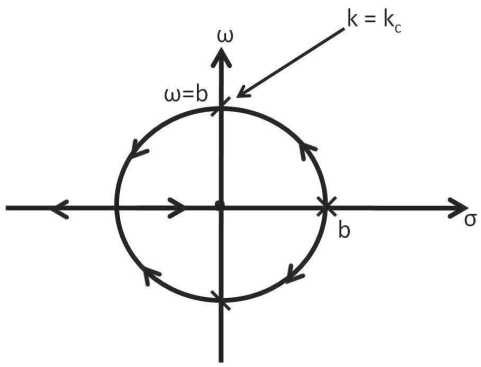

Fig. 2. Root locus for the associated linear system.

Using any relevant idea such as the calibration equation of the root locus [15], it is readily established that the locus branches pass into the left half plane as k passes through the value

$$k_c = \frac{\left[\sqrt{2}b\right]^2}{b} = 2b \tag{3}$$

Therefore, Lyapunov's theorem of the first approximation guarantees that the null state of the original nonlinear system is asymptotically stable for $k > 2b$. On the other hand for

$$k < 2b \tag{4}$$

a stable, almost sinusoidal oscillation in y at angular frequency

$$\omega = b \tag{5}$$

ensues. In order to demonstrate this we use Describing Function analysis and invoke an informal application of the Nyquist stability criterion [16].

Describing Function analysis, which has been justified under conditions which apply here [17], is based on the assumption that the input to the nonlinear characteristic is very closely approximated by the expression

$$e = E_m \sin \omega t \tag{6}$$

The signal u is then periodic with period $\frac{2\pi}{\omega}$, but very non-sinusoidal. The influence of all Fourier series components at angular frequencies 3ω, 5ω, 7ω,...etc is almost completely filtered out by the $G(s)$ block. (Odd harmonics only are encountered here due to the "inverse repeat" property of u, subject to the chosen $f(e)$ being an odd function of e). The

fundamental component of u has no phase shift relative to e, a feature which is also guaranteed by $f(e)$ being an odd function of e. It is denoted by

$$u_f = U_m \sin \omega t \tag{7}$$

By standard Fourier analysis, U_m is given by

$$U_m = \frac{\omega}{\pi} \int_0^{\frac{2\pi}{\omega}} f\left(E_m \sin \omega t\right) . \sin \omega t . dt \tag{8}$$

From symmetry considerations, this may be written as

$$U_m = \frac{4\omega}{\pi} \int_0^{\frac{\pi}{2\omega}} f(E_m \sin \omega t) . \sin \omega t . dt \tag{9}$$

In the range $0 \leq f \leq \frac{\pi}{2\omega}$, the quantity

$$x = E_m \sin \omega t \tag{10}$$

varies monotonically with t, and so no ambiguity is introduced by changing the variable of integration from t to x. The integral is transformed to

$$U_m = \frac{4}{\pi E_m} \int_{x=0}^{E_m} \frac{f(x).x}{\sqrt{E_m^2 - x^2}} dx. \tag{11}$$

This leads to

$$U_m = \frac{-4}{\pi E_m} \int_0^{Em} f(x) . \frac{d}{dx} \sqrt{E_m^2 - x^2} . dx,$$

which can be integrated by parts to give

$$U_m = \frac{4}{\pi E_m} \left\{ -f(x) \sqrt{E_m^2 - x^2} + \int \sqrt{E_m^2 - x^2} \frac{df}{dx} . dx \right\} \Bigg|_0^{E_m} \tag{12}$$

In our problem we have, for $x > 0$,

$$f(x) = kx + gx^2$$

giving

$$U_m = \frac{4}{\pi E_m} \int_0^{E_m} \sqrt{E_m^2 - x^2} . \left[k + 2gx\right] dx$$

which leads to

$$U_m = kE_m + \frac{8g}{3\pi} E_m^2 \tag{13}$$

where integrals 132 and 133 on page 52 of Rektorys [18] have been used. The Describing Function (DF) is defined as the effective gain of the nonlinearity for sinusoidal inputs, i.e.,

$$DF = \frac{U_m}{E_m} = k + \frac{8g}{3\pi} E_m \tag{14}$$

Harmonic balance around the loop now gives $DF.G(j\omega) = -1$, i.e.,

$$G(j\omega) = -\frac{1}{DF} \tag{15}$$

Equation (15) is illustrated on Fig. 3 for $k < 2b$, i.e. $-\frac{1}{k} < -\frac{1}{2b}$. At the point of intersection of the two loci,

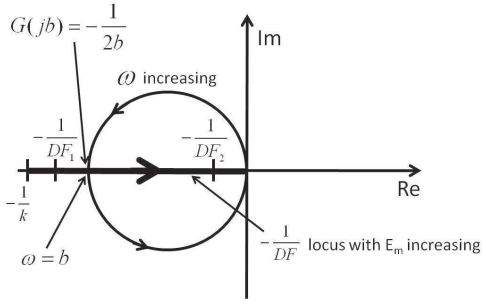

Fig. 3. Exploration of equation (15) on the $G(s)$ plane.

$$-\frac{1}{k + \frac{8g}{3\pi} E_m} = -\frac{1}{2b}$$

i.e.

$$E_m = \frac{\left[2b - k\right] 3\pi}{8g} \tag{16}$$

Despite the approximations inherent in the use of Describing Function analysis, (16) predicts that an almost sinusoidal oscillation exists for exactly the same range of values of k as predicted by root locus analysis applied to the linearized system.

The stability of the oscillation may be established by invoking the Nyquist criterion, with $-\frac{1}{DF}$ taking the role of the critical point [10]. If N is the number of clockwise encirclements which the complete Nyquist diagram of $G(s)$ makes of the point $-\frac{1}{DF}$, and if N_o is the number of poles of $G(s)$ in the right half plane, and if N_c is the number of closed loop eigenvalues in the right half plane, then, according to the Nyquist criterion,

$$N_c = N_o + N \tag{17}$$

In this case $N_o = 2$, and the *complete* Nyquist diagram of $G(s)$ consists of two counter-clockwise traverses around the frequency response locus drawn on Fig. 3.

If we take a value $E_m < \frac{[2b-k]3\pi}{8g}$, the $-\frac{1}{DF}$ point (labeled $-\frac{1}{DF1}$) lies outside the complete Nyquist diagram, thus giving $N = 0$ and

$$N_c = N_o = 2 \tag{18}$$

For this value of E_m, the loop is unstable, having two eigenvalues (a complex conjugate pair) in the right half plane. The oscillation amplitude E_m is therefore growing and the $-\frac{1}{DF}$ point is moving to the right.

For $E_m > \frac{[2b-k]3\pi}{8g}$, the $-\frac{1}{DF}$ point, (labeled $-\frac{1}{DF2}$) lies inside the Nyquist diagram, with $N = -2$ (two counterclockwise encirclements) giving $N_c = 0$. The loop is asymptotically stable and the assumed oscillation is dying out i.e. E_m is decreasing. Thus, the $-\frac{1}{DF}$ point is moving to the left. The intersection described by (16) therefore represents a stable oscillation at angular frequency b radians per second.

We now pose the question: how is this oscillation to be quenched? In deep brain stimulation (DBS) a charge-balanced periodic signal $d(t)$ of the type sketched on Fig. 4 is injected into the loop. The frequency $\frac{1}{T}$ is chosen to lie well above

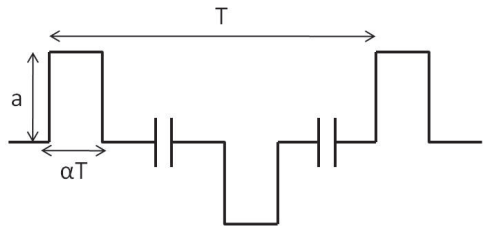

Fig. 4. The DBS waveform

the passband of $G(s)$. In order to invoke a technique known as the Equivalent Nonlinearity [10], $d(t)$ is considered to be injected at the input to the nonlinearity, as shown on Fig. 5.

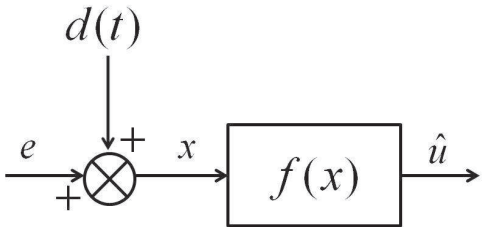

Fig. 5. Injection of the DBS waveform

It is shown in [10] and papers leading up to it, that the output y of the $G(s)$ block behaves as if the combination of the original nonlinearity $f(x)$ and the DBS signal $d(t)$ were replaced by the equivalent nonlinearity shown on Fig. 6.

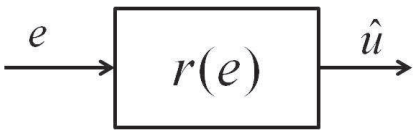

Fig. 6. The equivalent nonlinearity $\hat{u} = r(e)$, where $\hat{u}$ is the average value of u over a DBS cycle, for a given value of e.

Because of the requirement on the frequency of the DBS signal, it is valid to consider e constant over a DBS cycle. Then, x spends a fraction α at $e + a$, a fraction α at $e - a$, and a fraction $1 - 2\alpha$ at e. Thus we have

$$r(e) = \alpha.f(e + a) + \alpha.f(e - a) + [1 - 2\alpha].f(e) \qquad (19)$$

Since $f(x)$ is an odd function of x, it follows very simply that $r(e)$, the mean value of e over a dither cycle, is an odd function of e. Thus, we need only evaluate $r(e)$ for $e \geqslant 0$ and the whole function is determined.

From Fig. 1 we have

$$f(e) = ke + ge\,|e| \qquad (20)$$

and this gives, for $0 \leqslant e \leqslant a$,

$$\begin{aligned} r(e) &= k\left[\alpha(e+a) + \alpha(e-a) + (1-2\alpha)e\right] \\ &+ g\left[\alpha(e+a)^2 - \alpha(e-a)^2 + (1-2\alpha)e^2\right] \\ &= \left[k + 4\alpha ga\right].e + g\left[1-2\alpha\right]e^2 \end{aligned} \qquad (21)$$

Similarly, for $e \geq a$ we obtain

$$r(e) = ke + g.e^2 + 2\alpha ga^2 \qquad (22)$$

It is very easy to show that these two expressions for $r(e)$ are equal at $e = a$, and also that their slopes $\frac{dr}{de}|_{e=a}$ are equal, so that the two expressions merge seamlessly.

The small signal gain is

$$\left.\frac{dr}{de}\right|_{e=0} = k + 4\alpha ga \qquad (23)$$

The important feature of this is that the small signal gain is increased by DBS injection. The root locus on Fig. 2 shows that for

$$k + 4\alpha ga > 2b \qquad (24)$$

the system is asymptotically stable, and so the critical value of a for extinction of the oscillation is

$$a_c = \frac{[2b-k]}{4\alpha g} \qquad (25)$$

We have a series of n data points (a_{c_i}, α_i) from Benabid *et al*. [1]. In the case that strict equality does not apply in (25), an error measure may be formed as

$$E = \sum_{i=1}^{n}\left[a_{c_i} - \frac{[2b-k]}{4\alpha_i g}\right]^2 \qquad (26)$$

The possibility is now explored of choosing k and g to minimize E and get the closest fit to Benabid's data. With the notation

$$A = \sum_{i=1}^{n}\frac{1}{\alpha_i^2} = 213420.15$$

$$B = \sum_{i=1}^{n}\frac{a_i}{\alpha_i} = 4356.81 \qquad (27)$$

the condition $\frac{\delta E}{\delta k} = 0$ gives

$$Ak + 4Bg = 2bA \qquad (28)$$

The condition $\frac{\delta E}{\delta g} = 0$ gives

$$8bBg - 4Bgk + 4bAk - Ak^2 = 4b^2A \qquad (29)$$

Substituting (28) into (29) gives (28) again.

Thus, there is only one condition obtained for the two parameters k and g. This means that, for example k may be chosen arbitrarily in the range $0 < k < 2b$ and g is then given by

$$g = \frac{[2b - k]A}{4B} \tag{30}$$

In order to illustrate the procedure, we select the following data points from Benabid *et al.* [1], noting that they employ a fixed pulse width $\alpha T = t_p$, giving

$$\alpha = t_p \nu \tag{31}$$

with $t_p = 60 \times 10^{-6}$s and ν denotes frequency in Hz.

TABLE I
DATA POINTS FROM BENABID *et al.* [1]

α_i	0.0032	0.0041	0.006	0.0077	0.0093	0.12
a_{c_i}	6.5	4.86	3.14	2.8	2.2	2

We select $b = 10\pi$ radians per second, corresponding to a 5Hz oscillation, in the Parkinsonian tremor band, normally between 3 and 8Hz. Choosing $k = 18\pi$, there results

$$g = \frac{[20\pi - 18\pi]A}{4B} = 76.95 \tag{32}$$

The corresponding curve of a_c vs. α, drawn from (25) is shown on Fig. 7, along with the data points from Table 1. The fit could hardly be better.

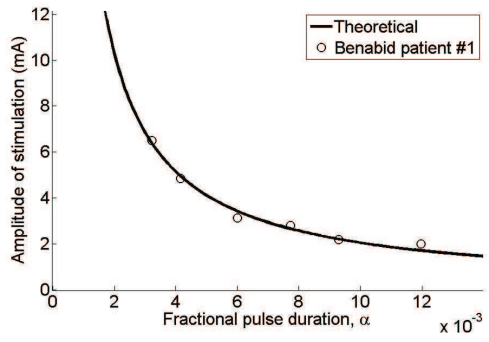

Fig. 7. The critical DBS amplitude for quenching the oscillation, along with data points from [1].

In order to show that the oscillation has indeed been stably quenched, it is necessary to demonstrate that the conditions shown on Fig. 8 apply (i.e. that $\left|-\frac{1}{DF}\right|$ decreases as E_m increases).

By following exactly the same procedure as in the earlier describing function calculation, but replacing $f(x)$ by $r(e)$, invoking appropriate integrals from p.520 of Rektorys [18], we derive the following. For $0 \leqslant E_m \leqslant a$,

$$DF = DF_a = [k + 4\alpha g a] + \frac{8g}{3\pi}[1 - 2\alpha].E_m \tag{33}$$

and for $E_m \geqslant a$,

$$DF = DF_a|_{E_m = a} + DF_b \tag{34}$$

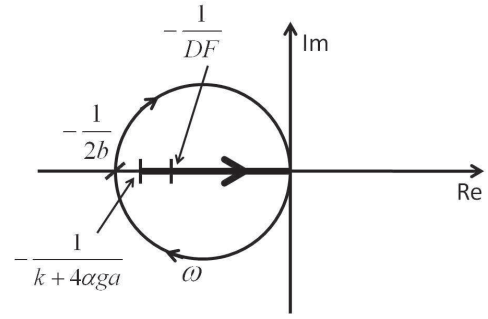

Fig. 8. Nyquist stability argument for the equivalent nonlinearity.

where

$$\begin{aligned} DF_b &= \frac{2ka\sqrt{E_m^2 - a^2}}{\pi E_m^2} + k\left[1 - \frac{2}{\pi}.\arcsin\left(\frac{a}{E_m}\right)\right] \\ &+ \frac{4ga^2\sqrt{E_m^2 - a^2}}{\pi E_m^2} + \frac{8g}{3\pi E_m^2}\left[E_m^2 - a^2\right]^{\frac{3}{2}} \\ &+ \frac{8\alpha g a^2\sqrt{E_m^2 - a^2}}{\pi E_m^2} \end{aligned} \tag{35}$$

A plot of DF vs. E_m is shown on Fig. 9. Fig. 9 emphasizes

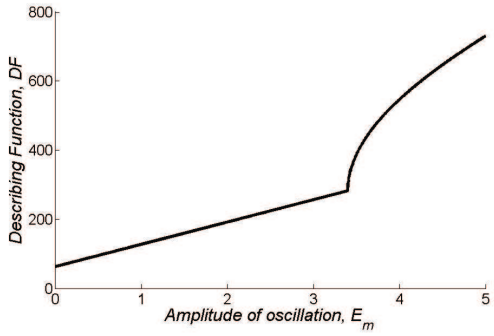

Fig. 9. DF vs. E_m for the equivalent nonlinearity, for $g = 76.95$, $\alpha = 0.006$, $a = 3.40$ and $k = 18\pi$.

that

$$DF(0) = [k + 4\alpha g a] \tag{36}$$

and that all the other terms in equations (33) and (35) are positive, increasing monotonically with Em. This shows that the situation sketched on Fig. 8 applies. Any initial $E_m > 0$ decays to zero, so that the $-\frac{1}{DF}$ point settles at $-\frac{1}{k+4\alpha g a} > -\frac{1}{2b}$, within the domain of asymptotic stability.

III. CONCLUSIONS

We have explored a second-order, non linear neural mass type model to represent the generation of pathological oscillations in functional units of the basal ganglia of the brain in Parkinson's Disease. Using several concepts from control theory, most notably the concept of the Equivalent Nonlinearity, we have been able to relate the critical amplitude of

DBS needed to quench the oscillation, to the fractional pulse-width of the rectangular, charge-balanced waveform used. By minimizing a quadratic error index we have determined the parameters of the model which will give best fit to experimental results given by Benabid *et al.* [1]. The results are in agreement with a suggestion made by Benabid [13], that one of the mechanisms of action of DBS could be "excitation of inhibitory pathways that lead to functional inhibition, mimicking the effect of lesioning of the stimulated structures". A very interesting point is that the critical DBS amplitude needed to quench the pathological oscillations is inversely proportional to fractional pulse-width. This means that the power for quenching, drawn from the battery in the stimulator, is also inversely proportional to the fractional pulse-width. At present, the patient has to undergo chest surgery, at two to three-yearly intervals, to replace the stimulator when its battery is approaching exhaustion, so it is clearly desirable to minimize power drawn from the stimulator battery. This would be achieved by using the largest value of pulse width possible, i.e. $\alpha = 0.5$, resulting in pure square-wave stimulation. However, clinical requirements, which do not appear to be clearly established yet, must determine the actual maximum pulse-width tolerable.

REFERENCES

[1] A. Benabid, P. Pollak, D. Hoffmann, C. Gervason, M. Hommel, J. Perret, J. de Rougemont, and D. Gao, "Long-term suppression of tremor by chronic stimulation of the ventral intermediate thalamic nucleus," *The Lancet*, vol. 337, no. 8738, pp. 403 – 406, 1991, originally published as Volume 1, Issue 8738.

[2] E. Moro, R. J. Esselink, J. Xie, M. Hommel, A. L. Benabid, and P. Pollak, "The impact on parkinson's disease of electrical parameter settings in stn stimulation," *Neurology*, vol. 59, no. 5, pp. 706–713, 2002.

[3] M. Rizzone, M. Lanotte, B. Bergamasco, A. Tavella, E. Torre, G. Faccani, A. Melcarne, and L. Lopiano, "Deep brain stimulation of the subthalamic nucleus in parkinson's disease: effects of variation in stimulation parameters," *Journal of Neurology, Neurosurgery & Psychiatry*, vol. 71, no. 2, pp. 215–219, 2001.

[4] P. E. O'Suilleabhain, W. Frawley, C. Giller, and R. B. Dewey, "Tremor response to polarity, voltage, pulsewidth and frequency of thalamic stimulation," *Neurology*, vol. 60, no. 5, pp. 786–790, 2003.

[5] M. Rosenblum and A. Pikovsky, "Delayed feedback control of collective synchrony: an approach to suppression of pathological brain rhythms," *Phys. Rev. E*, vol. 70, p. 041904, Oct 2004.

[6] Gillies, D. Willshaw, and Z. Li, "Subthalamic pallidal interactions are critical in determining normal and abnormal functioning of the basal ganglia," *Proceedings of the Royal Society of London. Series B: Biological Sciences*, vol. 269, no. 1491, pp. 545–551, 2002.

[7] S. W. Johnson, "Rebound bursts following inhibition: how dopamine modifies firing pattern in subthalamic neurons," *The Journal of Physiology*, vol. 586, no. 8, p. 2033, 2008.

[8] A. A. Kuhn, A. Tsui, T. Aziz, N. Ray, C. Brucke, A. Kupsch, G.-H. Schneider, and P. Brown, "Pathological synchronisation in the subthalamic nucleus of patients with parkinson's disease relates to both bradykinesia and rigidity," *Experimental Neurology*, vol. 215, no. 2, pp. 380 – 387, 2009.

[9] D. Plenz and S. T. Kital, "A basal ganglia pacemaker formed by the subthalamic nucleus and external globus pallidus," *Nature*, vol. 400, pp. 677 – 682, 1999.

[10] R. J. Simpson and H. M. Power, "Applications of high frequency signal injection in non-linear systems," *International Journal of Control*, vol. 26, no. 6, pp. 917–943, 1977.

[11] A. de Paor and M. Lowery, "Analysis of the mechanism of action of deep brain stimulation using the concepts of dither injection and the equivalent nonlinearity," *Biomedical Engineering, IEEE Transactions on*, vol. 56, no. 11, pp. 2717 –2720, nov. 2009.

[12] C. Davidson, M. Lowery, and A. de Paor, "Application of non-linear control theory to a model of deep brain stimulation," in *Engineering in Medicine and Biology Society,EMBC, 2011 Annual International Conference of the IEEE*, Aug. 30 - Sept. 3 2011 2011, pp. 6785 –6788.

[13] A. L. Benabid, "What the future holds for deep brain stimulation," *Expert Review of Medical Devices*, vol. 4, no. 6, pp. 895–903, 2007.

[14] F. L. da Silva, A. van Rotterdam, P. Barts, E. van Heusden, and W. Burr, "Models of neuronal populations: The basic mechanisms of rhythmicity," in *Perspectives in Brain Research*, ser. Progress in Brain Research, M. Corner and D. Swaab, Eds. Elsevier, 1976, vol. 45, pp. 281 – 308.

[15] A. de Paor, "The root locus method: famous curves, control designs and non-control applications." *International Journal of Electrical Engineering Education*, vol. 37, no. 4, p. 344, 2000.

[16] H. M. Power and R. J. Simpson, *Introduction to dynamics and control*. McGraw-Hill (London and New York), 1978.

[17] A. R. Bergen and R. L. Franks, "Justification of the describing function method," *SIAM Journal on Control*, vol. 9, no. 4, pp. 568–589, 1971.

[18] K. Rektorys, *Survey of applicable mathematics*. M.I.T. Press, 1969.